Wet Etching and Surface Analysis of Chemically Treated InGaN Films

N. Karar,[a,c,z] R. Opila,[a] and T. Beebe, Jr.[b]

[a]Department of Materials Science and Engineering and [b]Department of Chemistry and Biochemistry, University of Delaware, Newark, Delaware 19716, USA

This paper discusses the performance of different wet chemical etchants on InGaN. It is shown that certain etchants can be used to chemically etch and remove appreciable amounts of InGaN even though the etch rate is not as high as observed for other III-V materials. The performance of etchants studied here were (i) two different ratios of HF, HNO_3, (ii) cyclic usage of NH_4OH followed by HCl, (iii) hot H_2SO_4 and H_3PO_4 mixture, and (iv) conc. NH_4OH. The etched surfaces have then been analyzed by x-ray photoelectron spectroscopy (XPS). Different etch residues were observed on the top surface. These results suggest an alternative to reactive plasma etching or photo-enhanced electrochemical etching of InGaN type materials. Based on the observed performance of the etchants studied, it was also possible to segregate the surface cleaning protocols and etchants.
© 2011 The Electrochemical Society.   [DOI: 10.1149/1.3574036] All rights reserved.

It is well known that in semiconductor materials and device fabrication, the important issues are materials' purity, growth, defect control, lithography, etching, contact formation, and device performance.[1,2] Among these, etching is an important process in which the grown material is required to be partially removed using specific patterns for subsequent doping, metalization, device structure formation, etc. In such processes, the rate of material removal has to be fast and repeatable. There is another associated process, in which the top layer of a material is cleaned before subsequent growth by removing a few angstroms and associated top layer contaminants. In this cleaning process, it is essential that the top layers are removed with care and the least amount of material is wasted. Thus, this chemical cleaning process has to be one with a slow material removal rate and with the least amount of interfering residues.

Such etching and cleaning may be done by electrochemical, wet chemical methods, reactive ion or sputter ion cleaning.[3] Electrochemical processes are not always very selective while removing materials and often require very tight control over bias voltages and currents. Wet chemical etching is a method of removing the top layer of a material in a solvent leading to its dissolution in the reaction medium. Often the etchants are a combination of acids or a combination of bases. In wet chemical methods, with proper calibration, it is possible to retain better material crystalline quality of the etched material and by controlling the concentration of chemicals in the reaction, the material removal rate can also be rigorously controlled. However in all etch steps, residues from etching steps are present; these need to be understood to evaluate the likely effects on the subsequent electrical properties of the device created. Wet chemical etching is thus often the preferred etching mechanism for lithographic process. It has often been seen that the traditional wet chemical or electrochemical processes may also have their other limitations, even though they are quite cost effective. Inability to get high etching rates or reaction induced surface passivation are some of the associated problems. Reactive ion etching and sputter ion cleaning, also called dry etching, was developed to overcome such problems. These processes have relatively higher etch/erosion rates, depending on the material being removed and the reactive or sputtering gas used. But they also have their own limitations in terms of higher defect and crystalline damage creation and residue implantation. Over the years, this dry etching procedure, has often become the standard operating procedure for certain specialized semiconductor industries.[4–6] Interestingly, wet chemistry continues to play an important role with RCA cleaning, chemical-mechanical polishing and copper deposition.

GaN and and associated materials are quite hard and reports of their wet etching are few,[7] with most reports preferring the dry method, even though it requires large capital investments.[4] However, the reported sputtering rates for GaN and related materials are also quite low and thus sputter etching is also time consuming. Photo-chemical and light induced electro-chemical etching techniques are other etching alternatives currently available for InGaN/GaN related materials.[8] In this context, we discuss the possibilities of etching InGaN/GaN type materials using wet chemical methods. The choice of acidic and basic mixtures to be used is an issue when an unknown material is to be wet chemically etched. There were literature reports on the use of etchants like (i) mixture of hot conc. H_2SO_4 and H_3PO_4 at 250°C (Ref. [9]); (ii) HCl; (iii) NH_4OH (Ref. [10]); but the usage and performance analysis of these last two in succession to combine the oxidizing and then the reducing features together was not envisaged earlier; that has been done here; (iv) usage of HF and HNO_3 mixture based (isotropic and anisotropic) etchants was based on one of the authors' past experience of working on GaSb based materials.[11] The etching performance of these chemical mixtures were then compared. X-ray photo electron spectroscopy (XPS) of the etched samples were performed to know the chemical contaminants present after the etch so that future results of electrical measurements can be appropriately correlated. This also gave information on the chemical bonding environments for Ga, In, N, and O on the surface. Such an analysis, using the similarities of an earlier report[12] will also help assign the XPS spectra.

Experimental

GaN and InGaN samples were prepared by organo-metallic chemical vapor deposition/epitaxy (MOCVD/MOVPE) process, with sapphire (Al_2O_3) as a substrate material. The growth details are briefly the following: a base layer of undoped GaN was grown on the sapphire to a thickness so that the surface growth defect density stabilized and epitaxial layer growth was achieved. A semi-insulating GaN layer was grown on top of this layer to isolate future electronic structures. The total GaN layer thickness was at least 2000 nm or more. Often the GaN thickness was double of this. This buffer layer was required to get an appropriate lattice matching for the subsequent InGaN/GaN based active layers. Active semiconductor layers based on p and n type InGaN were grown on top of this (Fig. 1).[13] The In content was about 17% or so. This active layer thickness varied from 150 to 450 nm or so, depending on the type of doping profile and structure needed.

As stated above, the objective here is to show the relative efficacy of different chemical etching processes on the top active InGaN layer (Fig. 1). The etchants studied are (i) anisotropic hydrofluoric acid (HF) having one part HNO_3, 69.8%, one part HF 49% and three parts of de-ionized water (H_2O), sourced from a Millipore water system), (ii) isotropic hydrofluoric acid (HF), (having nine parts of HNO_3, 69.8%, and one part HF 49%), (iii) first NH_4OH

[c] Permanent address: National Physical Laboratory, New Delhi, 110012, India.
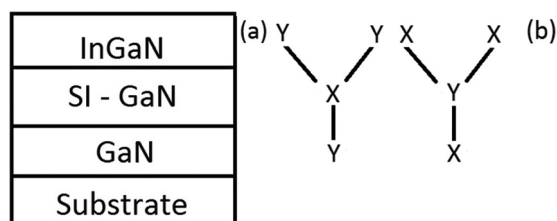[z] E-mail: nkarar78@gmail.com

Figure 1. (a) A schematic diagram of the InGaN samples being etched; (b) A schematic diagram of the different bonds, associated with etched fcc InGaN structure; X represents Ga or In; Y represents N or an etch related radical like OEx with E being an element like H, N, P, F or Cl and x is a real positive fraction less than one.

soln. followed by concentrated hydrochloric acid (conc. HCl 37.5%), (iv) mixture of sulfuric acid (H_2SO_4, 96.9%) and phosphoric acid (H_3PO_4, 85%) (3:1 ratio), heated to a hot-plate temperature of 250°C, and (v) concentrated ammonia solution (NH_4OH soln. 29.5%). All the chemicals were sourced from Fisher Scientific and used as is.

The etched surface morphology was observed using a Nikon Eclipse TE 2000-S optical microscope and the resulting images were analyzed using the open-source Image-J software. The sample surface was also observed using a Talystep surface profilometer as well as a Vecco Digital Instruments Nanoscope IV Multi-mode Atomic Force Microscope (AFM) in taping mode using a Nanoscope 6.12 Software. Fifty micrometre square of sample surface were considered for investigation in each case. However, such topographic images are omitted here for brevity and only the surface roughness values have been stated (Table I).

We tried out different polymers, including colorless nail polish, and Shiplay photoresists as mask materials. The samples were cured to increase the adhesion to the surface. In etching using HF, at the end of the etch process, the polymers had got totally removed, due to etching under the polymers and reaction with the polymers too. So properly calibrating the etch rate became an issue. The etch rate calibration was then done by partially dipping the samples into the etch solution so that a measurable step could be formed.

In that respect, mask materials like colorless nail polish, and Shiplay photoresists could significantly withstand the Ammonia solution/HCl etch cycles for a long time and may be considered as an appropriate mask for this etch. However, we were unable to find an appropriate polymer based mask for the HF related wet etchants. It will be another totally different field of research to identify the appropriate polymer and its mean molecular weight/chain length from among polyethylene, difluoro-ethylene, and tryfluoro-ethylene, to see which one of these can withstand the etchant for the etching times required while slowly getting degraded in its own chain length and bond structure so that it becomes effectively removable at the end of the etch with the common solvents available in the laboratory.

Table I. Table showing the etch rates of different etchants on InGaN/GaN and their surface roughness values after etching; Unetched surfaces had RMS roughness values of about 27 nm. This table is a partial one as the surface cleaning related etchants (ammonia and phosphoric acid) are evidently slow etchants, and their associated erosion rates were not calculated.

Etchant	rate (μm/min)	RMS roughness (nm)
Anisotropic HF	0.13	18.1
Isotropic HF	0.30	23.7
Conc. NH_4OH and conc. HCl	0.04 (cycle)	20.4
Conc. H_2SO_4 and H_3PO_4	low	16.8
NH_4OH solution only	low	4.7

In order to distinguish an etched depth with surface roughness, HF based etching was done for half an hour so that after washing the etched area was visible to the eye under a microscope. In the case of cyclic etching, each cycle consisted of dipping the sample first in ammonia solution, washing it and then dipping it in HCl, each for 10 min duration. This cycle was repeated 10 times so that an appreciable amount of material was etched away and the etched thickness could be measured without any major uncertainty. In the case of cyclic etching, the associated number presented implies a minutes' cycle etch (Table I).

Surface chemical spectra was taken using a VG Escalab 220i-XL X-Ray Photoelectron Spectroscopy (XPS) system with a double crystal based monochromatic Al source using a pass energy of 20 eV for the high resolution scans with a step interval of 0.1 eV. The related data analysis and peak fitting was done using CasaXPS software[14] and finally plotted using Origin software. The components of the raw elemental XPS scans were analyzed using a Shirley background, with all components having an equal full width at half maximum (FWHM) values and a profile 80% Gaussian and 20% Lorentzian curves. The number of assigned components if different than the number stated here lead to a difficulty in getting the obtained experimental profile. The XPS peak assignment was based on accepted standard literature reports.[15–26] GaP was used as a standard sample to understand the GaN XPS peaks better, since in Ga based compound semiconductor samples, very often there is interference of Ga related XPS and Auger peaks with other elemental peaks over a wide binding energy (BE) range.

Results and Discussion

Anisotropic HF etchant.— The details of different elemental peaks found after the etching processes, the different related bonds and associated peaks, their correlation and related analysis are presented below. Traces of organic contaminants in the form of carbon C 1s peaks were visible at 284.6 eV (Fig. 2a). This C-H bond based peak position was also used for a calibration of the other elemental peak positions.

The best possible peak fit for Ga 2p3/2 (Fig. 3a) suggests presence of three components at 1116.8, 1118.1 and 1119.7 eV respectively, corresponding to Ga-N bonds related peaks, the last peak is possibly Ga-oxyfluoride ($GaOF_x$) related, the latter coming from the etch process.[23,24] The Ga-N related peak is relatively weaker due to the chemically etched surface. This fitted average Ga-N related peak and the normal peak for Ga-O are a little off from their usual position, possibly due to the presence of the oxyfluoride component at the surface (Table II). Depending on the value of x, and the relative concentration of HF in the reactant, the relative position of the $GaOF_x$ peak may shift a bit. As evident from above, Ga 2p3/2 has a high binding energy and thus correspond to low kinetic energy electrons. Thus, the above data came primarily from the upper part of the etched surface as opposed to the Ga 3d5/2 peaks which have a very low binding energy and hence corresponds to electrons with higher kinetic energy.

Ga 3d5/2 peak is in close proximity to In 3d5/2 peaks.[20,25] The best fitted peak components of the overall profile were separated based on reported results for Ga 3d5/2 and experimental data obtained after a comparison with data from a standard GaP sample (not shown here). The Ga 3d5/2 had two peak components at 18.7 and 19.8 eV corresponding primarily to Ga-N and the Ga-ON_x or Ga-O related component. It is difficult to separate the latter two here. The latter component is unlikely to be from Ga-OF_x. The In 4d5/2 associated peak at 16.5 eV is attributed to In-N (Fig. 4a). The In 4d5/2 could not be separated into components. These peaks correspond to deeper sample depths.

The observed change in the relative intensity of Ga-N, Ga-O or for Ga-OF_x related peak components with respect to other components for the "surface" and "bulk" part of the sample, i.e. a comparison of relative intensities of the Ga 2p3/2 and Ga 3d5/2 components shows that etching processes are only surface sensitive. Thus based
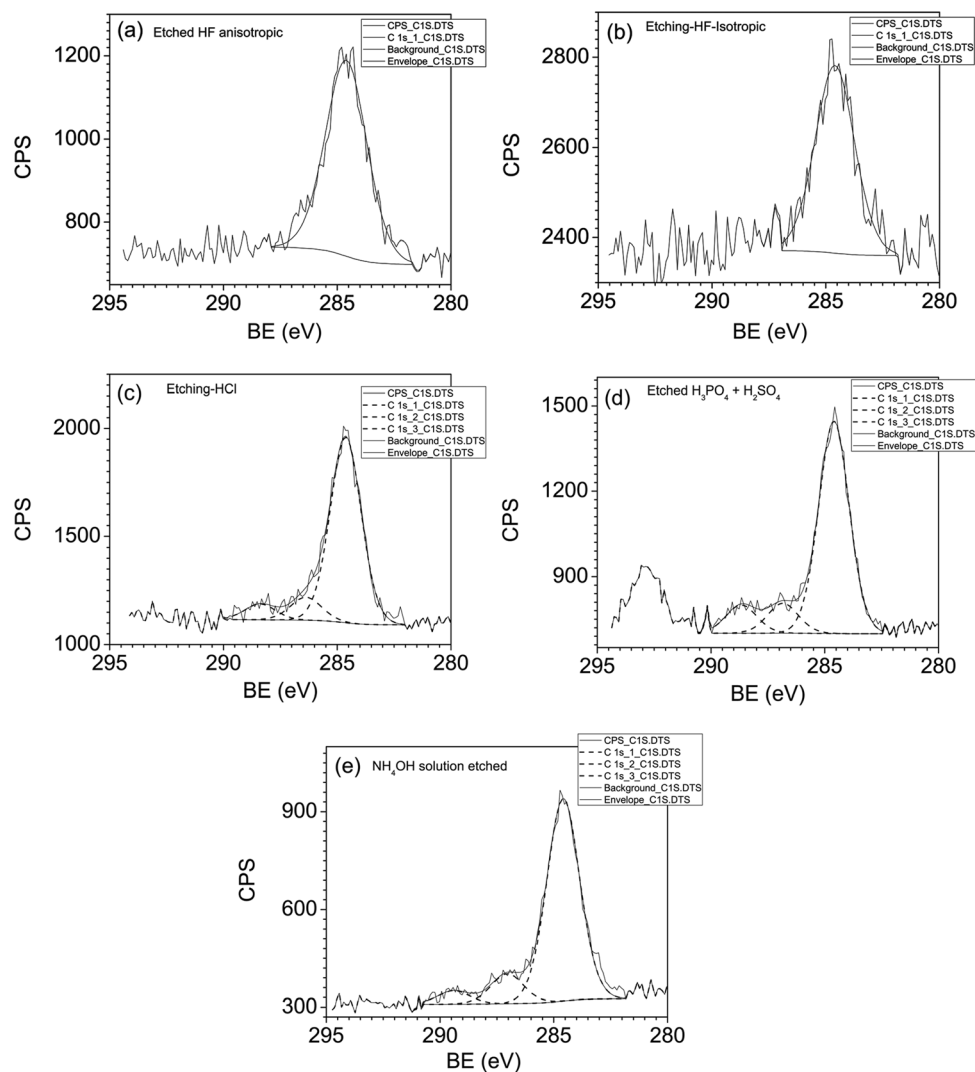
Figure 2. C 1s peak profile of different etched InGaN samples.

on above data, it may be said that the number of expected Ga Auger peaks can be taken as two or at most three. Any other fitted component in that contour may be safely considered to be from other elements.

In 3d5/2 had two major peak components at 443.8 and 444.9 eV corresponding to In-N bonds and In-O or In related oxyfluoride (In-OF_x) components, respectively (Fig. 5a). Since In 3d5/2 has high kinetic energy, the spectrum will be dominated by the bulk. These fitted peaks were also a little shifted from their expected positions due to the formation of the oxyfluoride component at the surface and our inability to separate the two (Table II).

A broad peak is observed at around 398 eV. This peak has two major constituents, one for the Ga LMM Auger lines and the other is for N 1s photoelectrons (Fig. 6a).[21,22] There were two resolved peak components from Ga Auger lines corresponding to electrons with moderate kinetic energies—these were distinguished after comparison with data from a standard GaP sample. This standard GaP sample had no peaks for N 1s but two Ga LMM Auger lines for Ga-N and surface oxidation related Ga-O, respectively. These Auger components were from surface of the material and correspond to the associated chemical states. Thus these have a correlation to the different Ga 2p3/2 or Ga 3d5/2 peak components observed in the sample. These two components are quite broad and correspond to Ga-N and Ga-O/GaOF$_x$; it was difficult to fit a third component here due

to the profile contour. Based on the type of etching process used, the number of Ga Auger peak components varied in each case. The number of Ga Auger peak components also correlate to the number of Ga 2p3/2 and Ga 3d5/2 peak components. The N 1s peak components were best fit at 397.1 and 398.9 eV. The other remaining components were appropriate Ga Auger lines. The peak at 397.1 eV is from N-Ga/N-In bonds. A comparison to an earlier report on the analysis of N 1s core level shifts in silicon oxynitride ($SiON_x$) (Ref. 12) shows that a possibility of $GaON_x$/Ga-$(NO_3)_3$ formation from the etch process is quite likely here too. In that case, the higher binding energy component, i.e. the smaller peak at 398.9 eV may correspond to the oxynitride component. The known electronegativity values for Ga is 1.6, for In it is 1.7, for N it is 3 and for O it is 3.5 (Refs. 27 and 28); thus it is most likely that due to the low difference in the electronegativity values for Ga and In, separate peaks for Ga and In are unlikely; but there may be a peak corresponding to O, due to its distinctly greater electronegativity.

The oxygen O 1s peak for this sample could not be resolved into components corresponding to difference between oxides and hydroxides of the metal Ga or In or for any oxyfluoride component as well, in part due to the weak signal of the O 1s peak (Fig. 7a).[26] Traces of the HF etchant were visible as an XPS peak of F 1s at 685.1 eV.[18,19] But it is not possible to further resolve this peak from Ga-F/In-F or any oxyfluoride component due to its low intensity.
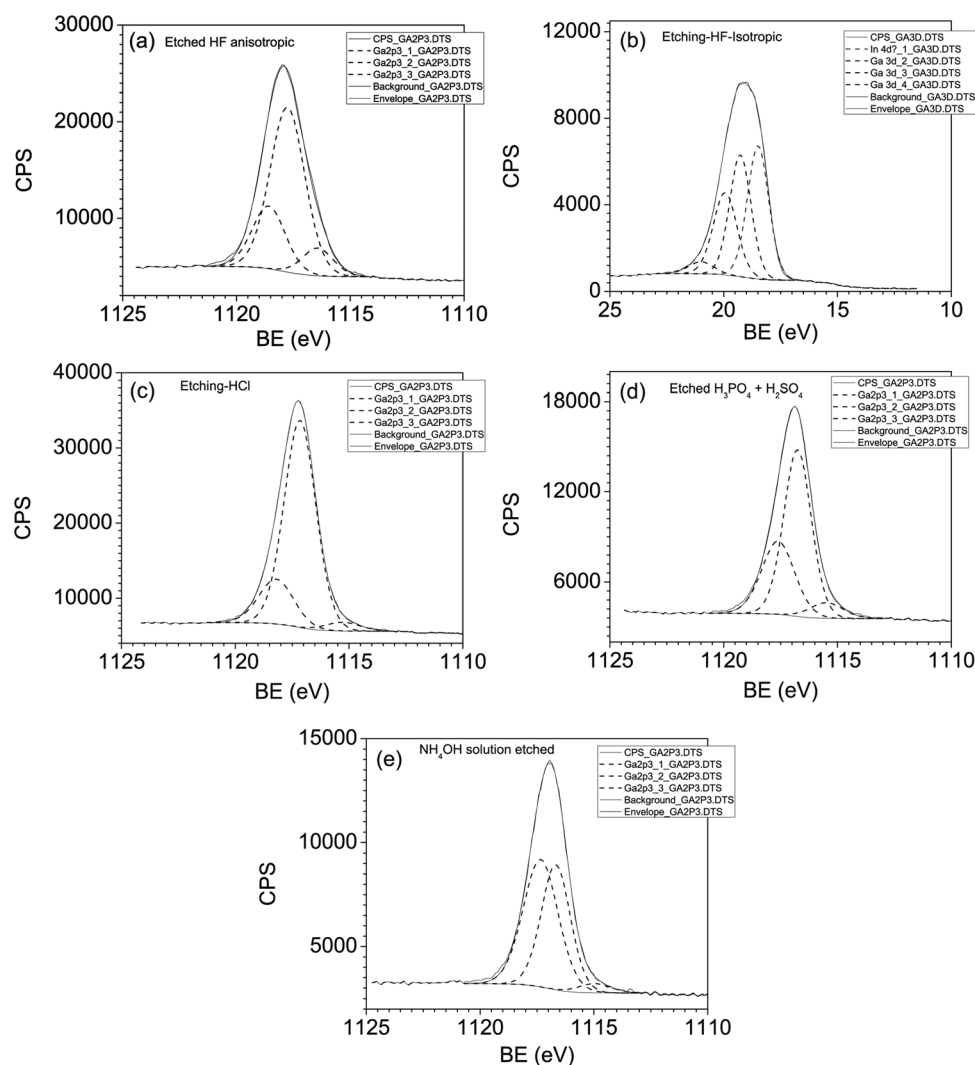
Figure 3. Ga 2p3/2 peak profile of different etched InGaN samples.

This HF based etching of InGaN sample also revealed two unknown low intensity peaks at 566.4 and 574.eV, which may correspond to incorporation of chromium (Cr 2p) from the Al_2O_3 sapphire substrate by diffusion during the high temperature growth process (peaks not shown here for brevity). Based on the above observation, where chromium diffusing was observed after etching of the original material, this etch was thought to be a moderately fast wet etch process. Its quantification may be beneficial for any future etching

related process applications. The calibrated etch rates for this etchant at room temperature was 0.13 μm/min

Isotropic HF etchant.— A single carbon C 1s peak at 284.6 eV suggested presence of trace ambient contaminants (Fig. 2b).

The Ga 2p3/2 peak profile shows four related components at 1115.3, 1116.7, 1117.6, 1119 eV corresponding to Ga-N, Ga-O, Ga-$(NO_3)_3$/GaON$_x$ and Ga-F/oxyfluoride (Ga-OF$_x$) respectively

Table II. A table based on the above analysis and discussion showing the different XPS peak positions (within ±0.2 eV) of different ion components; E refers to any non-halogen element, e.g., P, H, N etc. and x is a fraction; if E is a halogen, the related binding energy values are higher; the O-and OE$_x$ related peaks are not always distinguishable separately in each sample.

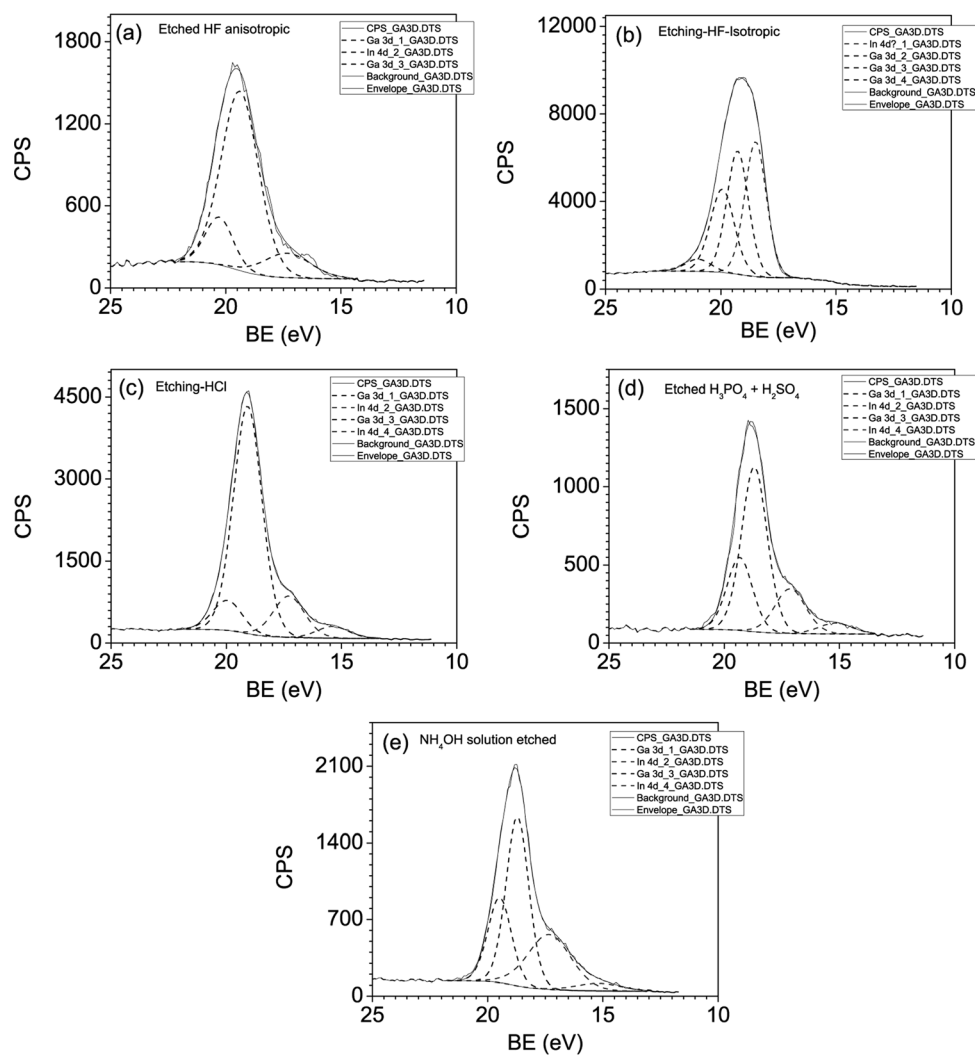|	Components	Peak positions (eV)	Ga 3d5/2	Components	Peak positions (eV)
Ga 2p3/2	Ga-N	1115.1		Ga-N	18.7
	Ga-O	1116.8		Ga-O	19.2
	Ga-OE$_x$	1117.8		Ga-OE$_x$	19.6
In 3d5/2	In-N	441	In 4d5/2	In-N	15.2
	In-O	443.8		In-O	17.1
	In-OE$_x$	444.9		In-OE$_x$	17.4
N 1s	Ga-N/In-N	397	O 1s	Ga-O/In-O	530.8
	Ga-ON$_x$/In-ON$_x$	398.7		Ga-OE$_x$	532.2

Figure 4. Ga 3d/In4d peak profile of different etched InGaN samples.

(Fig. 3b). The effect of change in the relative fluoride ion ratio in the etch solution on the peak position of Ga-OF$_x$ is notable.

The uniqueness of this etch was that four Ga 3d5/2 peak components were visible at 18.4, 19.1, 19.8, and 20.9 eV possibly corresponding to Ga-N, Ga-O, Ga-(NO$_3$)$_3$/GaONx and Ga-F/oxyfluoride (Ga-OF$_x$) respectively (Fig. 4b). There are also two oxygen peaks to suggest possible presence of NO$_3$. The Ga-(NO$_3$)$_3$/GaON$_x$ peaks were visible separately due to the higher NO$_3$ ion content in the etch solution. A comparison of the relative peak intensity changes for the different peak components related to Ga 2p3/2 and Ga 3d5/2 shows that the top layer contains relatively more intense peaks for the oxides while at the more deeper parts of the sample, the nitride peak component is predominant.

This InGaN sample does not show any presence of In 4d5/2 peaks, or presence of any In 3d5/2 peaks either. This suggests that all the InGaN layers was etched away leaving only the bottom GaN seed layers instead.

There were two N 1s peaks at 397 eV and 398.5 eV corresponding to Ga-N and Ga-(NO$_3$)$_3$/GaON$_x$ bonds respectively (Fig. 6b). The other peaks correspond to four Auger lines for the Ga peaks discussed below. The oxygen O 1s peak for this HF etched sample had two components at 530.8 and 532.3 eV possibly corresponding to Ga-O and Ga-NO$_3$/GaON$_x$ respectively (Fig. 7b).[26] The similar In related components could be merged into the Ga related oxide spectra. Traces of the HF etchant in terms of an XPS peak of F 1s at 684.9 eV were also visible.

This HF etched InGaN sample also showed two low concentration peaks at 563.8 and 572.3 eV, which may correspond to a incorporation of chromium from the sapphire substrate.

In this sample, the upper InGaN layer was etched away due to the higher NO$_3$ ion content in the etchant. The role of HF is to convert the top layer to insoluble GaF$_3$/InF$_3$, while HNO$_3$ converts the fluoride to soluble gallium nitrate (Ga(NO$_3$)$_3$)/indium nitrate (In(NO$_3$)$_3$). Essentially, the amount of the fluoride in the medium remains constant, with HF acting more like a catalyst. The relative amount of NO$_3$ ions in the solution determines the extent of etching. The calibrated etch rates for this etchant at room temperature was 0.30 μm/min.

Conc. NH$_4$OH and conc. HCl in succession.—This etch process was developed after observing the report of three independent groups[10,16,17] and thereafter appropriately modifying the process. Traces of extra carbon peaks, other than the C 1s at 284.6 eV were observed, and corresponds to presence of adventitious contaminants (Fig. 2c).

The sample had three Ga 2p3/2 peak components at 1115.4, 1117.1 and 1117.8 eV corresponding to Ga-N bonds, Ga-O and possibly from GaOCl$_x$ respectively (Fig. 3c). The peak for Ga-O was strongest due to the nature of the etch process and the surface sensitive nature of this etch.

Ga 3d5/2 region of this sample, which corresponds to signals from the deepest part within the material had peaks at 19.1 and 20
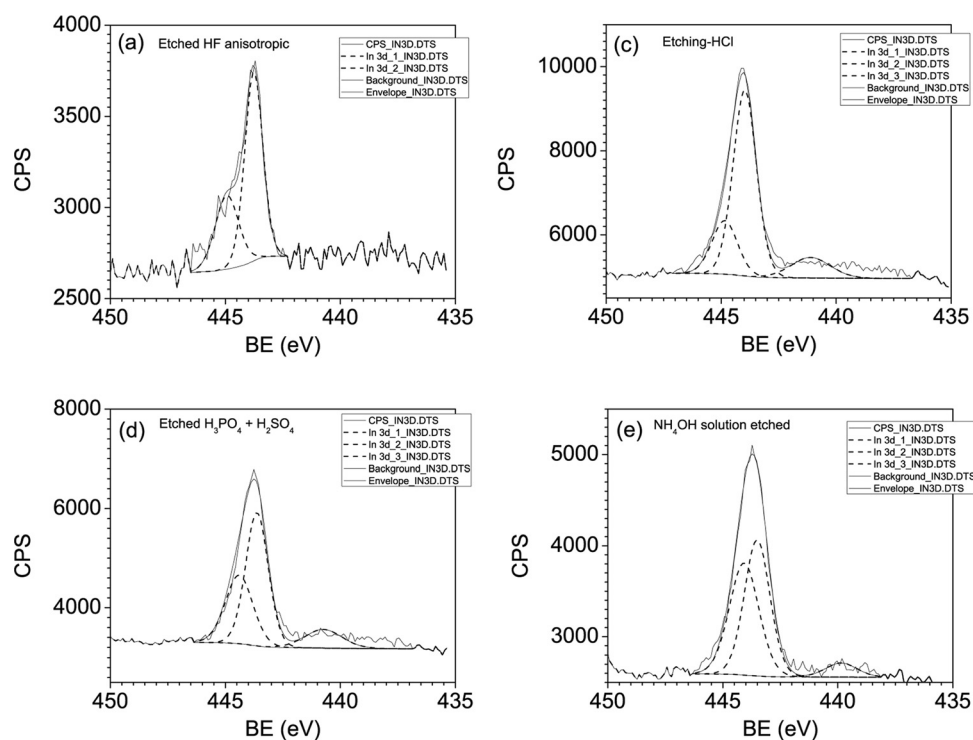
Figure 5. In 3d5/2 peak profile of different etched InGaN samples; date from (b) was omitted due to complete In removal.

eV due to Ga-N bonds and Ga-O respectively (Fig. 4c). Looking at the center of the Ga-O peak here (Table II), it is felt that there may also be an unresolved Ga-OCl$_x$ component within it. This again suggests on the sensitive nature of the etch process. In 4d5/2 showed two peaks at 15.2 and and 17.4 eV corresponding to In-N bonds and In-O. The relative difference in the heights may correspond to the relative differences of reactivity of In and Ga with oxygen.

In 3d5/2 has three components at 442, 444.1, and 445.4 eV corresponding to In-N bonds, In-O and possibly InOCl$_x$ respectively (Fig. 5c). The difference in the number of surface related In 3d5/2 and volume related In 4d5/2 peak components is due to the surface sensitive nature of the etch process. Nitrogen has two N 1s peaks at 396.8 and 397.6 eV corresponding to Ga-N/In-N bonds and H/OH type bond formation respectively. There were also three Ga Auger peaks in the same area corresponding to Ga-N, Ga-O and GaOClx respectively (Fig. 6c). Oxygen 1s showed peaks at 530.8 eV from Ga-O/In-O and at 531.9 eV from GaOCl$_x$ (Fig. 7c). No peak component for Ga-OH could be separately identified, possibly due to the subsequent HCl related reaction. Cl 1s peaks are not shown here for brevity.

In this two step etch process, at first gallium oxide (Ga$_2$O$_3$) was formed using concentrated ammonia solution. This is in itself a limiting process as gallium oxide formation passivated the surface and stops further reactions. However, not much material is removed in this step as the oxide is in itself not very soluble. Thereafter, conc. HCl efficiently converted the gallium oxide to soluble gallium chloride, which was dissolved in the reaction medium. The top surface was then again oxidized for subsequent removal as a chloride and such number of cycles could be repeated as per requirement. This sample showed deep etching due to two the successive etching steps. A few μm could be etched by this process if used cyclically, with an etch rate of 0.04 μm/min. It is thus seen that wet chemical etching can also be a stand alone process for material removal of InGaN type materials. The uniqueness of this process was the two steps required, at first the oxide formation with a solution and then its removal. It is felt that such two step process of etching may be subsequently emulated for other materials as well, specially where a single step etching gets limited by a surface passivation layer.

After etching, two peaks corresponding to Cr 2p were also visible at around 574 and 565.3 eV in the form of two large humps due to the deep etching possible. These are possibly from Cr based impurities that out-diffuse from the sapphire substrate due to the sample growth temperature (spectra not shown here).

Conc. H$_2$SO$_4$ and H$_3$PO$_4$ at 250°C.—This process was essentially based on the report by Weyher et al.[9] and was used here for a comparison of the relative efficacy of different etchants. There were small adventitious trace contaminants other than the C-H peak at 284.6 eV along with a small peak for potassium K 2p3/2 -which possibly came from the glassware at the elevated etching temperature of 250°C (Fig. 2d).

There were three Ga 2p3/2 peak components at 1115.1, 1116.8 and 1118 eV corresponding to Ga-N bonds, Ga-O, and Ga-(PO$_3$)/Ga-OP$_x$ respectively (Fig. 3d). The Ga-O peak was relatively strong corresponding to the nature of the etch process.

Peak components of Ga 3d5/2 for Ga-N bonds at 18.7 eV and Ga-O/Ga-OP$_x$ at 19.3 eV were also visible. The slight change from the peak position for any likely Ga 3d5/2 for Ga-O may be noted (Table II). There were also two adjacent In 4d5/2 peak components at 15.1 and 17.1 eV corresponding to In-N bonds and In-(PO$_3$)/In-O respectively (Fig. 4d). The nature of this process ensured presence of relatively higher oxygen components on the surface.

In 3d5/2 has three perceptible components at 441, 443.8, 444.9 eV corresponding to In-N bonds, In-O and In-(PO$_3$)/In-OPx (Fig. 5d) respectively.

Nitrogen N 1s had peak components at 396.4 for Ga-N/In-N bonds and at 397.7 eV possibly for ON$_x$ bonds. The lower values here for the N 1s binding energy in Ga-N/In-N is possibly due to lack of any other ion in the bond. In the same region, there were three Ga Auger peaks corresponding to Ga-(PO$_3$), Ga-O and Ga-N respectively (Fig. 6d).

There was also the two O 1s components for Ga-O and Ga-(PO$_3$)/In-(PO$_3$) at 531.3 and 532.5 eV (Fig. 7d). There were traces of phosphorus P 2p3/2 at 133.3 eV possibly from the above etchant residues. The role of heated H$_3$PO$_4$ was to convert the surface to Ga(PO$_3$)$_3$ while the H$_2$SO$_4$ converted this phosphate to soluble
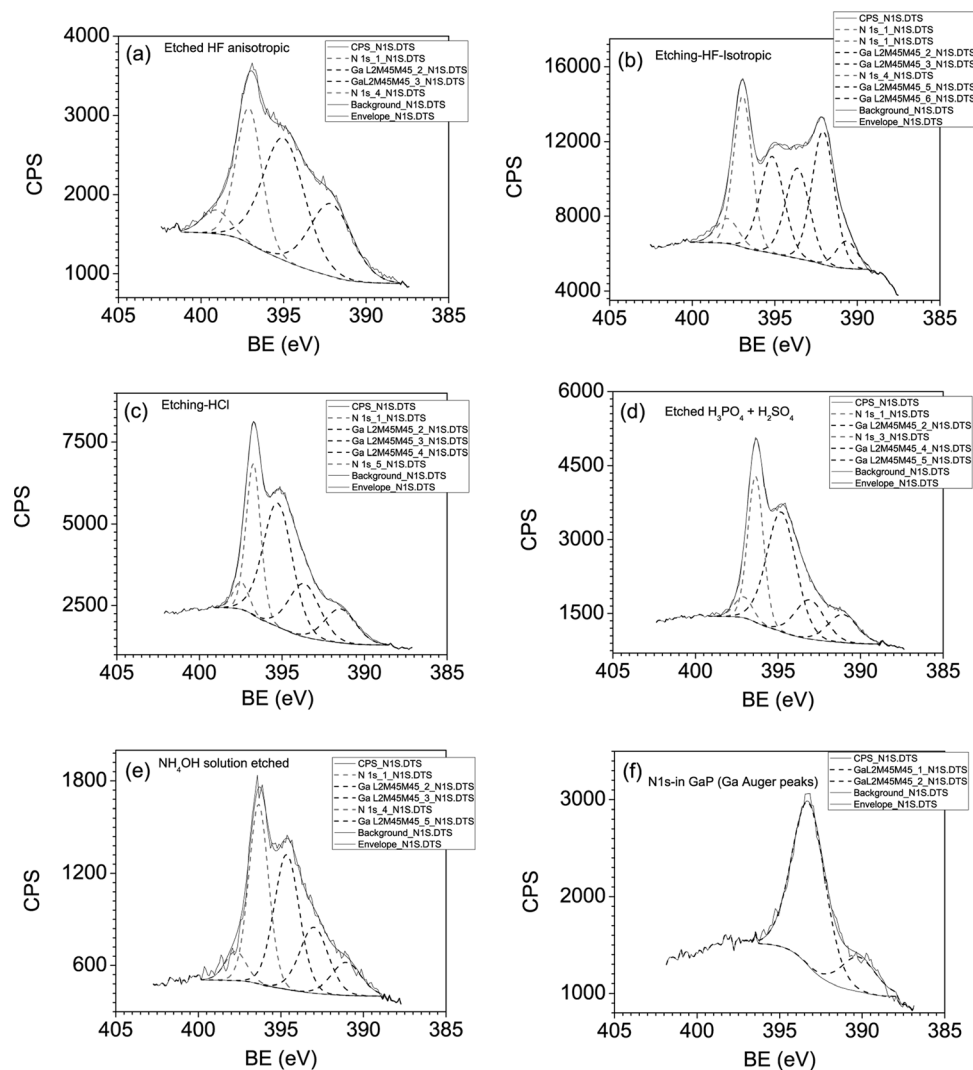
Figure 6. N 1s peak profile of different etched InGaN samples and from a standard GaP sample (f).

gallium sulfate. Here the etch rates were not calculated as this slow limiting process is essentially suitable only for surface cleaning.

NH₄OH solution only.—This etch solution was separately considered in order to understand its performance as a stand alone etchant. There were traces of adventitious contaminants other than the C 1s C-H peak at 284.6 eV (Fig. 2e).

The gallium Ga 2p3/2 had three resolvable components at 1114.9, 1116.9 and 1117.9 eV corresponding to Ga-N bonds, Ga-O, and possibly Ga-ON$_x$; these signals came mainly from the surface (Fig. 3e). The oxygen component was strong due to the nature of the etchant. Two Ga 3d5/2 peak components were visible at 18.7 and 19.5 eV corresponding to Ga-N bonds and Ga-O; the latter peak could not be further distinguished. There were also two related In 4d5/2 peak components in the same area at 15.2 and 17.3 eV related to In-N bonds and In-O respectively (Fig. 4e).

There were three perceptible indium In 3d5/2 peak components at 440, 443.7 and 445 eV corresponding to In-N bonds, In-O and In-ONx respectively (Fig. 5e).

Nitrogen N 1s had peak components at 396.4, 398.3 eV corresponding to Ga-N/In-N bonds and ON$_x$ bonds respectively; the slight shift of the peak due to higher presence of ON$_x$ may be noted. There were also three Ga Auger peaks in the same area corresponding to Ga-N, Ga-O, and Ga-OH respectively (Fig. 6e).

There were two perceptible oxygen O 1s peak components at 530.4 and 532 eV corresponding to Ga-O/In-O and GaON$_x$/InON$_x$

respectively from the usage of oxidizing etch NH4OH (Fig. 7e). The sole presence of ammonia solution and related reaction and identification of a separate Ga-ON$_x$ related peak resulted in a slightly different fitted O 1s peaks here (Table II). Gallium oxide (Ga$_2$O$_3$) related bond formation led to passivation of the top surface and limited further material removal. Here etch rates were not calculated as this slow process is suitable only for surface cleaning.

Other etching issues.—A detailed surface analysis using optical as well as atomic force microscopy on the different etched surfaces was done. The etch pits were visible for all etchants and in spite of the large number of areas and images considered for each type of etching, it is difficult to say that only a particular etchant is useful in revealing the etch pits, though the nature of the etch pits were seen to depend on the type of etchant. This is unlike the situation of other known III-V materials, where certain etchants are known to reveal etch pits much better than others. InGaN/GaN has a much higher defect density wrt other III-V materials. The effect of an etchant on a particular material is also dependent on the type of etchant under consideration, on the crystal structure of the material and relative erosion rate of different crystalline planes of that material. So a plane selective etchant for a certain material may not be that plane sensitive in another.

Though wet etching by cyclic ammonia/HCl is slower than the two HF based etchants studied, it is not so corrosive to remove the polymer masks as well. Often, etching is time barred, where after a
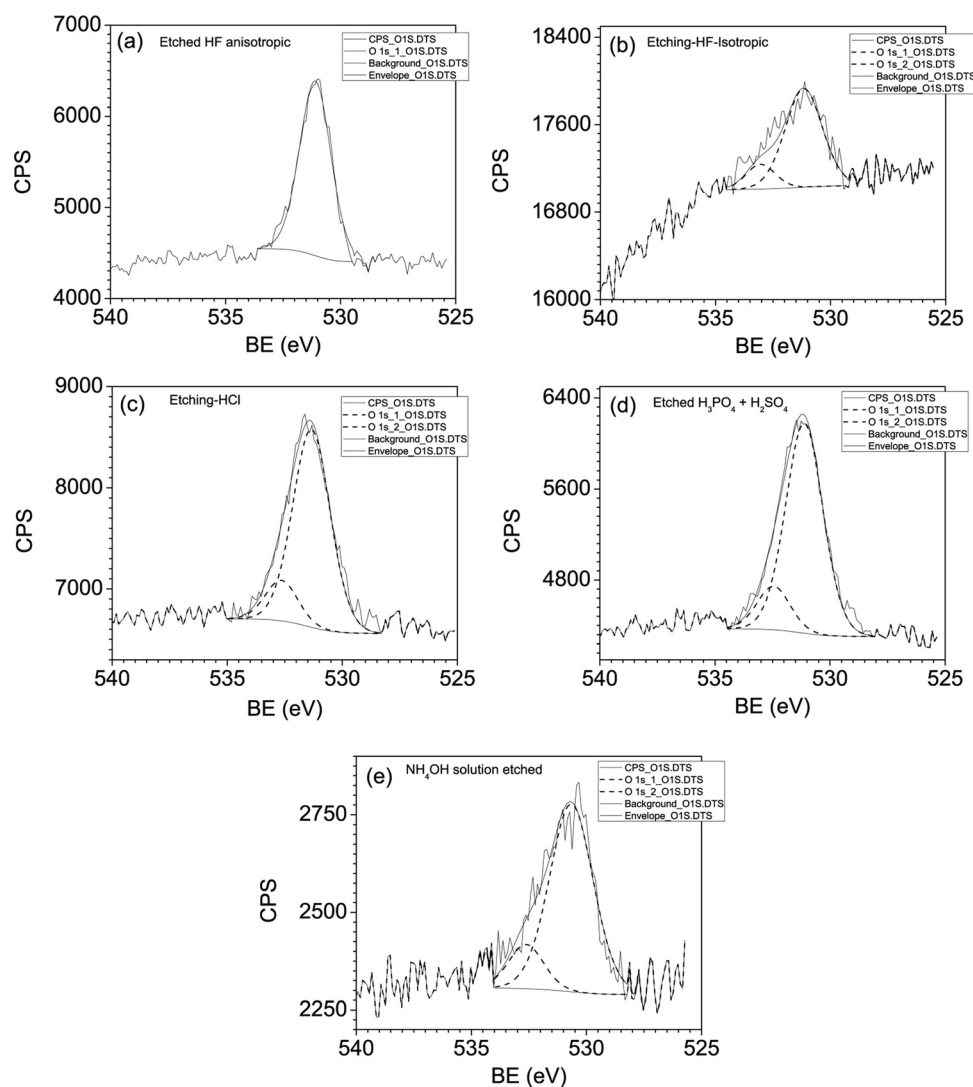
Figure 7. O 1s peak profile of different etched InGaN samples. The fluoro-oxide related peaks, if any, have not been accounted for.

while the etch process stops on its own. In this two step process, the passivating oxide formed in the initial step is removed in the next step. This is such a cyclic two step process, where effectively a good amount of material may be removed. Such a two step process may perhaps be replicated for other materials as well. It may be recalled that due to the time barring nature of many wet etch processes, sputter-etching processes became popular. Such ideas may thus revive interest in wet etching processes again. Usage of this process in low volume applications may be possible.

Conclusions

XPS results for different etched InGaN/GaN surfaces showed the chemical state of different surfaces after etching, including the different impurities present. This could be related to the efficiency of the etching process. A comparative analysis of different studied etchants shows that cyclic usage of conc. ammonia (NH_4OH) solution followed by conc. HCl is a "clean" etchant for removing InGaN/GaN layers. A similar two step etching process may be successful for other materials where etching is limited by surface passivation. HF and HNO_3 solution mixture was also successful as a relatively fast etchant. It was often possible to etch almost up to the base GaN layer. Etchants like ammonia (NH_4OH) solution alone or Conc. H_2SO_4 and H_3PO_4 mixture were good enough only for cleaning up the top layer. The etch rates were also calibrated. However,

compared to other III-V materials, the etching rate in GaN/InGaN is an order of magnitude less.

References

1. *Introduction to Nitride Semiconductor Blue Lasers and Light Emitting Diodes*, S. Nakamura and S. Chichibu, Editors, CRC, USA (2000).
2. Group III Nitride Semiconductor Compounds, B. Gill, Editor, p. 35, Oxford University, New York (1998).
3. Handbook of Semiconductor Wafer Cleaning Technology, W. Kern, Editor, Noyes Publications, USA (1993).
4. Handbook of Plasma Processing Technology, S. Rossnagel, J. Cuamo, and W. Westwood, Editors, Noyes Publications, USA (1990).
5. Y. Kawakami, A. Kaneta, L. Su, Y. Zhu, K. Okamoto, M. Funato, A. Kikuchi, and K. Kishino, J. *Appl. Phys.*, **107**, 023522, (2010).
6. M. Schuette and W. Lu, *J. Vac. Sci. Technol. B*, 25, 1870, (2007).
7. D. Zhuang and J. H. Edgar, *Mater. Sci. Eng. R*, **48**, 1, (2005).
8. A. Tamboli, M. Schmidt, S. Rajan, J. Speck, U. Mishra, S. DenBaars, and E. Hua, *J. Electrochem. Soc.*, **156**, H47, (2009).
9. J. L. Weyher, S. Lazar, L. Macht, Z. Liliental-Weber, R. Molnar, S. Muller, V. Sivel, G. Nowak, and I. Grzegory, *J. Crystal Growth*, **305**, 384, (2007).
10. R. Sohal, P. Dudek, and O. Hilt, *Appl. Surf. Sci.*, **256**, 2210, (2010).

11. N. Karar, S. Basu, and S. Sainkar, *J. Alloys Compd.*, **307**, 272, (2000).
12. J. Eng, I. Hubner, J. Barriocanal, R. Opila, and D. Doren, *J. Appl. Phys.*, 95, 1963, (2004).
13. N. Faleev, B. Jampana, O. Jani, H. Yu, R. Opila, I. Ferguson, and C. Honsberg, *Appl. Phys. Lett.*, **95**, 051915, (2009).
14. The Casa Cookbook, N. Fairley and A. Carrick, Editors, Acolyte Science, UK (2005).
15. Handbook of X-Ray Photoelectron Spectroscopy, J. Moulder, W. Stickle, P. Sobol, and K. Bomden, Editors, Physical Electronics Inc., USA (1995).
16. Y. Chang, H. Chiu, Y. J. Lee, M. Huang, K. Lee, M. Hong, Y. Chiu, J. Kwo, and Y. Wang, *Appl. Phys. Lett.*, **90**, 232904, (2007).
17. H. Lu, X. A. Cao, S. F. LeBoeuf, H. C. Hong, E. B. Kaminsky, and S. D. Arthur, *J. Crystal Growth*, **291**, 82, (2006).
18. A. Vajpai, S. Chua, S. Tripathi, and E. Fitzgerald, *Appl. Phys. Lett.*, **91**, 08311, (2007).
19. Y. Choi, J. Lim, Y. Kim, M. Kim, O. Seok, and M. Han, *ECS Trans.*, **25**(12), 117 (2009).
20. M. Toda, J. Yanagisawa, K. Gamo, and Y. Akasaka, *J. Vac. Sci. Technol. B*, **22**, 3012, (2004).
21. H. Hasegawa, T. Inagaki, S. Ootomo, and T. Hashizume, *J. Vac. Sci. Technol. B*, 21, 1844, (2003).
22. T. Nagata, G. Koblmller, O. Bierwagen, C. Gallinat, and J. Speck, *Appl. Phys. Lett.*, **95**, 132104, (2009).
23. S. Wolter, B. Luther, D. Waltemyer, C. Onneby, S. Mohneya, and R. Molnar, *J. Appl. Phys.*, **70**, 2156, (1997).
24. M. Toda, J. Yanagisawa, K. Gamo, and Y. Akasaka, *J. Vac. Sci. Technol. B*, **22**, 3012, (2004).
25. A. Siderenko, H. Peisert, H. Neumann, and T. Chasse, *Surf. Sci.*, **601**, 4521, (2007).
26. T. Hashizume, S. Ootomo, R. Nakasaki, and S. Oyama, and M. Kihara, *Appl. Phys. Lett.*, **76**, 2880, (2000).
27. http://www.thecatalyst.org/electabl.html, last accessed. 25th March, 2011.
28. D. Harris, *Quantitative Chemical Analysis*, 7th ed., W. H. Freeman and Company, USA (2007).